AGU PUBLICATIONS

Geophysical Research Letters

RESEARCH LETTER
10.1002/2014GL059989

Key Points:
- This study provides a new perspective on ENSO genesis
- Westerly wind bursts could be responsible for El Niño diversity
- This study improves our understanding and forecasting of ENSO

Correspondence to:
D. Chen,
dchen@sio.org.cn

Citation:
Lian, T., D. Chen, Y. Tang, and Q. Wu (2014), Effects of westerly wind bursts on El Niño: A new perspective, *Geophys. Res. Lett.*, *41*, 3522–3527, doi:10.1002/2014GL059989.

Received 25 MAR 2014
Accepted 9 MAY 2014
Accepted article online 15 MAY 2014
Published online 28 MAY 2014

Effects of westerly wind bursts on El Niño: A new perspective

Tao Lian[1], Dake Chen[1,2], Youmin Tang[1,3], and Qiaoyan Wu[1]

[1]State Key Laboratory of Satellite Ocean Environment Dynamics, Second Institute of Oceanography, State Oceanic Administration, Hangzhou, China, [2]Lamont-Doherty Earth Observatory, Columbia University, New York, New York, USA, [3]Environmental Science and Engineering, University of Northern British Columbia, Prince George, Canada

Abstract Daily observations from 1971 to 2010 reveal that every El Niño during this period was accompanied by congregated westerly wind bursts, suggesting a close relationship of these bursts with both "cold tongue" and "warm pool" El Niño events. With the addition of burst-like multiplicative noise to an intermediate ocean-atmosphere coupled model, it is shown that westerly wind bursts, by generating eastward equatorial surface currents and downwelling Kelvin waves, could be responsible for the existence of the warm pool El Niño and for the irregularity and extremes of the cold tongue El Niño. Whether these bursts give rise to one type of El Nino or the other depends on the timing of their occurrence relative to the phase of the recharge-discharge cycle of the equatorial upper ocean heat content.

1. Introduction

It has long been recognized that El Niño–Southern Oscillation (ENSO) is mainly a result of the ocean-atmosphere interaction in the tropical Pacific [e.g., *Bjerknes*, 1969], but there is still a considerable debate on the mechanisms that are responsible for the maintenance and variability of ENSO. Present theories can be generally grouped into two different frameworks. In the first framework, ENSO is regarded as a self-sustaining oscillation with its time scale determined by the recharge and discharge of the equatorial upper ocean heat content [e.g., *Wyrtki*, 1975; *Jin*, 1997; *Horii et al.*, 2012]. In the second framework, ENSO is considered as a highly damped oscillation with each event triggered by stochastic atmospheric noise [e.g., *Penland and Sardeshmukh*, 1995; *Newman et al.*, 2011]. The former appears to be consistent with the long-lead predictability of ENSO [*Chen et al.*, 2004; *Chen and Cane*, 2008], while the latter seems to explain the irregularity and different behaviors of ENSO.

One specific stochastic forcing implicated in the second framework is the westerly wind burst (WWB) in the tropical western and central Pacific [*Vecchi and Harrison*, 2000]. WWBs can lead to strong zonal currents, which can transport a large amount of warm water from the warm pool region to the central Pacific and can also produce downwelling Kelvin waves that propagate eastward and cause warming in the eastern Pacific [*McPhaden*, 1999]. Both of these processes favor the onset of El Niño events. In fact, WWBs were observed to occur in association with the onset of every significant El Niño over the past 5 decades [*McPhaden*, 2004]. It is further shown that WWB is not stochastic after all—there is a deterministic part of it modulated by the low-frequency sea surface temperature (SST) variation associated with ENSO [*Eisenman et al.*, 2005; *Gebbie and Tziperman,* 2009]. This implies that the two different theoretical frameworks of ENSO mentioned above could be reconciled within a unified framework.

Recent studies seem to indicate that El Niño events can be classified into two basic types: the canonical El Niño that has the largest variance in the eastern Pacific cold tongue region [*Rasmusson and Carpenter*, 1982] and a weaker warming pattern centered near the date line [e.g., *Ashok et al.*, 2007; *Kug et al.*, 2009]. These are also known as cold tongue El Niño (CTEN) and warm pool El Niño (WPEN), respectively. It has been suggested that the number of WPEN has increased relative to CTEN in the recent decades [*Lee and McPhaden*, 2010; *Yeh et al.*, 2009]. While the genesis of CTEN can be explained by classic ENSO theories [e.g., *Jin,* 1997], the mechanism of WPEN is still far from being fully understood. Interestingly, the zonal heat advection in the vicinity of the date line is considered to play a key role in the development of WPEN [*Kug et al.*, 2009], which we assume may well result from the equatorial jet flow driven by WWBs.

In this study, we first analyze the relationship of WWB with both CTEN and WPEN for the period 1971–2010 using observational data. Then we investigate the roles of WWBs in the generation processes of WPEN and

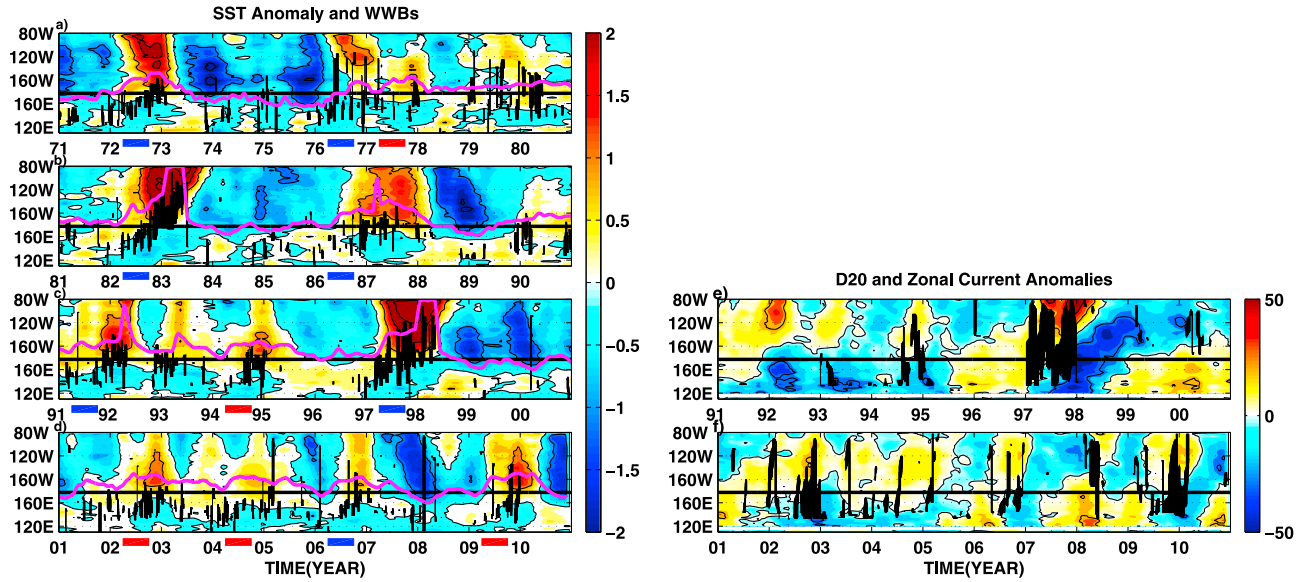

Figure 1. Evolution of observed variables along the equator. (left column) The SST anomaly (color and contour, unit in °C) with WWB (black lines) superimposed. The purple lines stand for 28.5°C isotherm, which is the monthly data filtered by a 1-2-1 filter. (right column) The D20 isotherm depth anomaly (color and contour, unit in meter) with zonal current anomalies greater than 0.25 ms^{-1} (black lines) superimposed (note that current data are not available before 1993). In Figure 1 (left column), CTEN and WPEN events are indicated by blue and red bars below abscissa, respectively.

CTEN by forcing an intermediate ocean-atmosphere coupled model with a set of WWB-like multiplicative noise. Our intention here is to provide a new perspective on WWB-ENSO relationship and to propose a mechanism for ENSO diversity using a framework that incorporates the effects of WWB into the classic recharge-discharge theory of ENSO.

2. Data and Model

The data sets used in this study include monthly reconstructed Hadley Centre Global Sea Ice and Sea Surface Temperature (HadISST) [*Rayner et al.*, 2003], daily surface wind speed from the National Centers for Environmental Prediction (NCEP) reanalysis [*Kalnay et al.*, 1996], weekly surface currents from satellite-derived Ocean Surface Current Analysis Real-time (OSCAR) [*Behringer and Xue*, 2004], and monthly 20°C isotherm (D20) data from the NCEP Global Ocean Data Assimilation System (GODAS) [*Saha et al.*, 2005]. The SST and wind data cover the period from 1971 to 2010, while the D20 and current data are based on the periods 1991–2010 and 1993–2010, respectively. Interannual anomalies of SST, surface current, and D20 are obtained by removing the climatological seasonal cycle and applying a low-pass 1-2-1 filter (similar to a 3 month running mean but with double weight on the central month) to reduce intraseasonal noise. WWBs are identified using the criteria of *Harrison and Vecchi* [1997], in which a WWB is defined as a westerly wind gust with a maximum speed of at least 7.0 ms^{-1} and a duration of 5 to 30 days during which the anomalous speed (obtained by removing the climatological seasonal cycle) exceeding 2.0 ms^{-1}.

An intermediate ocean-atmosphere coupled model [*Zebiak and Cane*, 1987] is employed to explore the effects of WWBs on ENSO. The model is set for the tropical Pacific (100°E–80°W, 30°S–30°N) with a horizontal resolution of 5.265° × 2° and a time step of 10 days. Two sets of model experiments are conducted. The first is a control run of 300 years with no external forcing aside from an initial kick, a 4 month westerly wind anomaly over the western equatorial Pacific as used by *Zebiak and Cane* [1987]. The second is a forced run, in which a set of idealized WWBs are added to the model wind stress field from year 101 to 300 of the control run. As pointed out by *Eisenman et al.* [2005], some model parameters need to be modified to prevent this model from becoming numerically unstable when adding strong anomalous wind stress. Therefore, we have reduced the coupling strength (drag coefficient) and the entrainment efficiency of the original model by 17.5% and 37.5%, respectively, and introduced a third-power nonlinear damping term in the model SST equation. With these modifications, the control run appears to be a weak, regular ENSO with a magnitude of about 0.5°C and a period of 5 years (as will be shown in Figure 2).

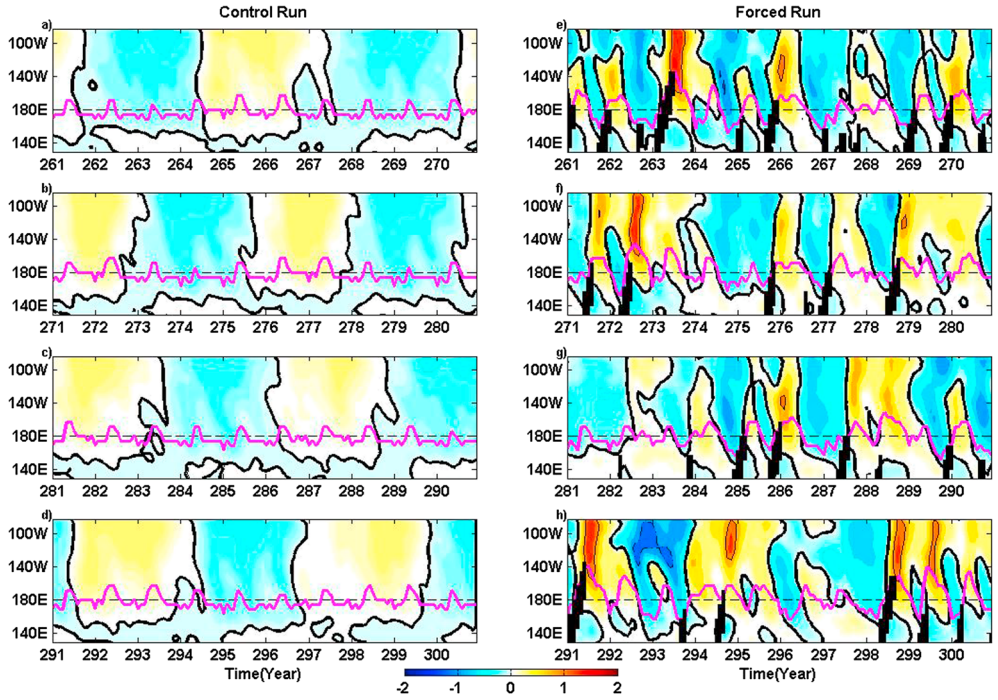

Figure 2. Evolution of model equatorial SST anomaly (color and contour) in (left column) the control run and (right column) the forced run with idealized WWB (black lines) superimposed. The units are the same as in Figure 1.

The idealized WWBs preserve a Gaussian shape at the equator [*Eisenman et al.*, 2005], and their initial longitude is set to 120°E, with a magnitude of 0.08 N m^{-2}. In order to account for the low-frequency modulation of WWBs by SST (as will be seen in the next section), a simplified scheme of the coupled SST-WWB relationship is applied [*Gebbie et al.*, 2007]. The initial triggering of a WWB is stochastic, but it is allowed to occur only when local SST exceeds 28.5°C. Once this condition is met, the WWB moves eastward at a speed of 0.5°/d, which is representative of the observed propagation speed. When the scheme produces no WWBs for 40 consecutive days, the center of the next WWB is set back to the initial longitude.

3. Results

The observed evolutions of the equatorial WWBs and SST anomalies (averaged from 5°S to 5°N) over the last 4 decades are shown in Figure 1 (left column). A striking feature is that all El Niño events, both CTEN and WPEN (as defined by *Yu and Kim* [2011]), were accompanied by congregated WWBs at their onset and mature phases, although WWBs also occurred at times without El Niño. Generally, WWBs are located west of the date line, but they tend to move eastward with the warm pool during El Niño [*Gebbie and Tziperman*, 2009]. Strong eastward surface currents are found to be associated with these WWBs (Figure 1, right column), indicating a possibly important role of the wind-driven equatorial jet in advecting warm water to the central Pacific. On the other hand, the interannual SST anomaly is apparently associated with the equatorial thermocline anomaly, especially in the far eastern Pacific where the climatological thermocline is relatively shallow (Figure 1, right column). In the WPEN years such as 1994–1995 and 2004–2005, the warming center was located just east of the date line and seemed to be mainly caused by zonal advection [*Picaut et al.*, 1997; *Kug et al.*, 2009]. In the CTEN years such as 1991–1992 and 1997–1998, however, the warm anomalies spread over the entire central and eastern basin, along with the eastward movement of WWBs and the equatorial zonal currents, as well as the large thermocline deepening in the cold tongue region.

The model-simulated SST anomalies from the control run and the WWB-forced run are compared in Figure 2 for the last 40 years of model experiments. In the control run, the model produces a rather weak and regular oscillation as mentioned earlier. The maximum SST anomalies always occur in the eastern equatorial Pacific, indicating that CTEN is the only type of El Niño that is produced by the control run of the model. An analysis of the surface layer heat budget (not shown) indicates that the changes in upwelling associated with the

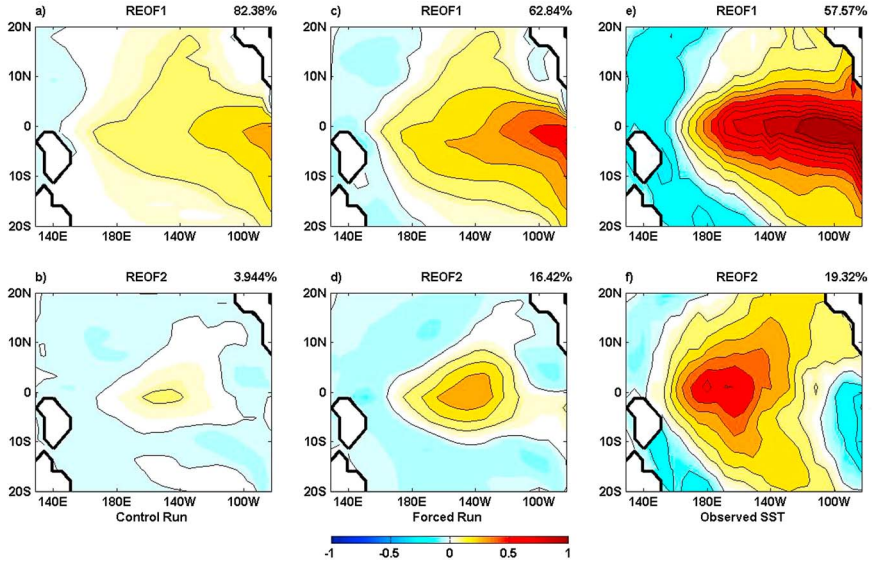

Figure 3. The first two REOF patterns of the tropical Pacific SST anomaly (unit in °C). (left column) Control run, (middle column) forced run, and (right column) observation. Contour interval is 0.1°C.

thermocline fluctuation play a crucial role in the ENSO cycle of the control run, which is consistent with the classic ENSO theory and the previous analyses of the standard Cane–Zebiak model [*Périgaud et al.*, 1997]. In the forced run, however, the interannual SST anomalies are irregular, and the model reproduces different "flavors" of El Niño. Strong warm events are accompanied by congregated, cross-date-line WWBs, with maximum warming located in the cold tongue region (CTEN). There are also some weak warm events located at the eastern edge of the western Pacific warm pool (WPEN), with WWBs confined to the western Pacific. The addition of the state-dependent WWBs not only causes irregularity of ENSO but also gives rise to two distinctively different types of El Niño.

To further demonstrate the effects of WWBs on ENSO, Figure 3 compares the dominant modes of the tropical Pacific SST variability from observation and the two model runs in the last 100 years. Here rotated empirical orthogonal function (REOF) analysis is used because it gives a more meaningful identification of the leading modes (especially the second mode) as compared to classical EOF analysis [*Lian and Chen*, 2012]. It is obvious that the first two modes of the observed SST represent CTEN and WPEN, respectively. The control run shows a single dominant mode that is similar to observed CTEN in spatial pattern but much weaker in magnitude. When WWB forcing is added, the first mode (CTEN mode) is significantly enhanced in amplitude as compared to the control run (0.6°C compared to 0.4°C), while the percentage of variance it explains is much reduced (62% compared to 82%). More importantly, the forced run shows a robust second mode with a spatial pattern quite similar to the observed WPEN (Figures 3d and 3f). This indicates that WWBs are responsible for the existence of WPEN and also for the strong events of CTEN in the model.

Based on the REOF patterns and the model SST evolutions, we define model CTEN events as those with an average SST anomaly in the far eastern equatorial Pacific (100°W–80°W, 5°S–5°N) exceeding one standard deviation (0.6°C) for more than three successive months and define model WPEN events as those with an average SST anomaly in the western equatorial Pacific (160°W–140°W, 5°S–5°N) exceeding 1 standard deviation (0.4°C) for at least three successive months. To identify the dominant processes for the development of each type of El Niño, Figures 4a and 4b show the area-averaged surface layer heat budgets of the composite WPEN and CTEN in the WWB-forced model run over a 3 month period before the maximum warming. Here the composites consist of 14 and 18 events for CTEN and WPEN, respectively, and the ratio of standard deviation to composite average is about 0.5. The relative importance of each term in the composite is quite consistent with that for individual events (not shown).

For WPEN (Figure 4a), the zonal and meridional advections are mainly responsible for its development, as expected from the eastward jet and equatorward convergence driven by WWBs. The vertical advection, which is directly related to thermocline variation in this model, is insignificant because the thermocline here

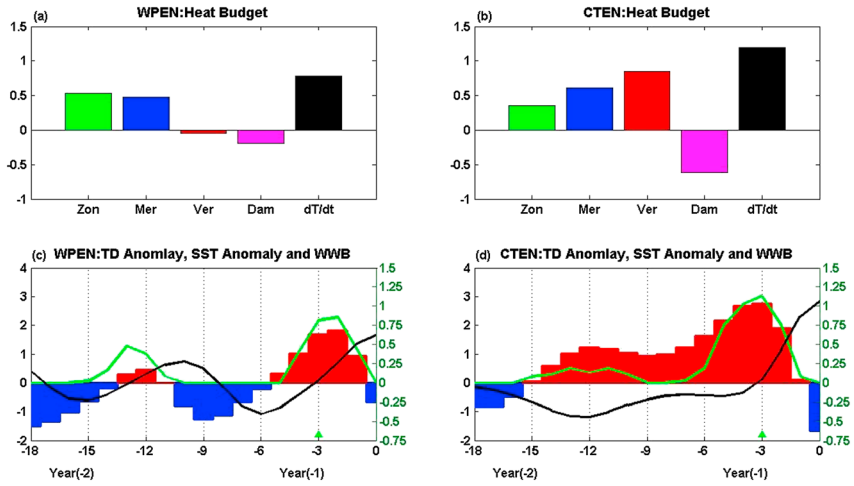

Figure 4. (top row) Surface mixed layer heat budget in the model for the composite (a) WPEN and (b) CTEN averaged over a 3 month period before the maximum warming. The green, blue, and red color bars denote the zonal, meridional, and vertical advection, respectively. The purple and black color bars are for the damping term and the total tendency. Unit is in °C/month. (bottom row) Evolutions of the zonally averaged equatorial thermocline depth (TD) anomaly (colors), the area-averaged SST anomaly (black curve), and the number of WWBs per month (green curve) for (c) WPEN and (d) CTEN. Units are in meter for TD and °C for SST. The left ordinate is for TD and WWB, and the right ordinate is for SST.

is relatively deep and thus is decoupled from SST. For CTEN (Figure 4b), however, all the three advective terms are important, with the vertical advection (thermocline deepening) being the dominant process. A more detailed analysis of the advective terms (not shown) reveals that it takes three steps to warm up the cold tongue region: first, a warming caused by reduced upwelling associated with the "recharging" of the equatorial heat content [*Jin*, 1997], then the warm water advection due to wind-driven surface currents, and finally the warming induced by the thermocline deepening related to the WWB-driven downwelling Kelvin waves.

To relate the occurrences of WPEN and CTEN to the basic recharge-discharge cycle of the equatorial heat content, Figures 4c and 4d display the evolutions of the composite WPEN and CTEN, respectively, along with the corresponding variations of the zonally averaged equatorial thermocline depth and the occurrences of WWBs, for a period of 18 months before the peaks of these events. In the case of WPEN (Figure 4c), there appear two groups of WWBs during the period, with the first starting from a discharged state (negative thermocline anomaly) and the second from a nearly neutral state. The former causes a small thermocline deepening and a very weak warming, while the latter produces a larger thermocline deepening and a warming that qualifies as a WPEN. Note that even for the latter, the thermocline deepening (vertical advection) is not the main cause of warming (as evident in Figure 4a) and that the SST response lags the WWB forcing by about 3 months. In the case of CTEN, there are also two groups of WWBs during the 18 month period, with the first starting from a nearly neutral state and the second from a recharged state (positive thermocline anomaly). The former causes a slight thermocline deepening and a delayed weak warming, while the latter produces a large thermocline deepening that leads to a strong CTEN. In general, a WPEN occurs when WWBs acting on a discharged or neutral phase of the basic cycle, while a CTEN takes place when WWBs appear during a recharged state.

4. Concluding Remarks

The relationship between the two types of El Niño and WWB is studied based on observational data and model experiments. Every El Niño over the past 40 years is observed to be closely associated with WWBs, with WPEN events related to the WWB-driven equatorial currents in the vicinity of the date line, and CTEN related to the thermocline deepening in the eastern equatorial Pacific as well as the WWB-driven currents. When WWB-like, state-dependent noise [*Eisenman et al.*, 2005] is added to an intermediate coupled model, the quasiperiodic, single-mode, weak ENSO cycle in the original model is drastically changed to an irregular oscillation characterized by distinctive CTEN and WPEN modes, with the former occasionally reaching a magnitude that is several times larger than in the model run without WWB forcing. The model results indicate that WWBs could be responsible for the genesis of WPEN and for the irregularity and extremes of CTEN.

It is then plausible to consider ENSO as a result of the interaction between a self-sustaining basic cycle dictated by the classic theory [e.g., *Zebiak and Cane*, 1987; *Jin*, 1997] and the WWB-type random noise that is partially modulated by ENSO itself [*Eisenman et al.*, 2005; *Jin et al.*, 2007]. The former provides the essential dynamical framework, while the latter produces the different flavors of ENSO. In particular, such a scenario may reconcile hotly debated issues related to the distinction and genesis of CTEN and WPEN. Since the basic ENSO is determined by the recharge-discharge cycle of the equatorial upper ocean heat content [*Jin*, 1997], the timing of noise acting on the cycle is crucial in determining which type of El Niño event may actually take place. When in a recharge phase, which favors the development of El Niño, WWBs can warm the central and eastern equatorial Pacific SST through combined effects of surface advection and downwelling Kelvin waves, leading to a strong CTEN event. When in a discharged or neutral phase, however, the equatorial thermocline is relatively flat, and it is not shallow enough in the eastern Pacific for the WWB-driven Kelvin waves to be effective, and thus, the impact of WWBs is limited to the warm advection near the date line, generating a relatively weak WPEN event.

Acknowledgments

The data sets used in this study include the HadISST (http://www.metoffice.gov.uk/hadobs/hadisst/), the NCEP reanalysis surface wind speed (http://www.esrl.noaa.gov/psd/data/gridded/data.ncep.reanalysis.surface.html), the OSCAR surface current (http://www.oscar.noaa.gov), and the GODAS thermocline depth (http://www.esrl.noaa.gov/psd/data/gridded/data.godas.html). Funding for this study is provided by the National Basic Research Program (2013CB430302), the Public Science and Technology Research Funds of Ocean (201105018), the National Natural Science Foundation of China (91128204, 41276030), and the "Air-Sea Interaction" International Research Project. Discussion with Ian Eisenman is helpful for the preparation of this manuscript. We also thank two anonymous reviewers for their helpful comments and suggestions.

The Editor thanks two anonymous reviewers for their assistance in evaluating this manuscript.

References

Ashok, K., S. K. Behera, S. A. Rao, H. Weng, and T. Yamagata (2007), El Niño Modoki and its possible teleconnection, *J. Geophys. Res.*, *112*, C11007, doi:10.1029/2006JC003798.

Behringer, D. W., and Y. Xue (2004), Evaluation of the global ocean data assimilation system at NCEP: The Pacific Ocean, Eighth Symposium on Integrated Observing and Assimilation Systems for Atmosphere, Oceans, and Land Surface, AMS 84th annual meeting, Washington State Convention and Trade Center, Seattle, Wash.

Bjerknes, J. (1969), Atmospheric teleconnections from the equatorial Pacific, *Mon. Weather Rev.*, *97*, 163–172.

Chen, D., and M. A. Cane (2008), El Niño prediction and predictability, *J. Comput. Phys.*, *227*, 3625–3640.

Chen, D., M. A. Cane, A. Kaplan, S. E. Zebiak, and D. J. Huang (2004), Predictability of El Niño over the past 148 years, *Nature*, *428*, 733–736.

Eisenman, I., L. Yu, and E. Tziperman (2005), Westerly wind bursts: ENSO's tail rather than the dog, *J. Clim.*, *18*, 5224–5238.

Gebbie, G., and E. Tziperman (2009), Predictability of SST-modulated westerly wind bursts, *J. Clim.*, *22*, 3894–3909.

Gebbie, G., I. Eisenman, A. Wittenberg, and E. Tziperman (2007), Modulation of westerly wind bursts by sea surface temperature: A semistochastic feedback for ENSO, *J. Atmos. Sci.*, *64*, 3281–3295.

Harrison, D. E., and G. A. Vecchi (1997), Westerly wind events in the tropical Pacific, 1986–95, *J. Clim.*, *10*, 3131–3156.

Horii, T., I. Ueki, and K. Hanawa (2012), Breakdown of ENSO predictors in the 2000s: Decadal changes of recharge/discharge-SST phase relation and atmospheric intraseasonal forcing, *Geophys. Res. Lett.*, *39*, L10707, doi:10.1029/2012GL051740.

Jin, F. F. (1997), An equatorial ocean recharge paradigm for ENSO. Part I: Conceptual model, *J. Atmos. Sci.*, *54*, 811–829.

Jin, F. F., L. Lin, A. Timmermann, and J. Zhao (2007), Ensemble-mean dynamics of the ENSO recharge oscillator under state-dependent stochastic forcing, *Geophys. Res. Lett.*, *34*, L03807, doi:10.1029/2006GL027372.

Kalnay, E., et al. (1996), The NCEP/NCAR 40-year Reanalysis Project, *Bull. Am. Meteorol. Soc.*, *77*, 437–472.

Kug, J.-S., F.-F. Jin, and S.-I. An (2009), Two types of El Niño events: Cold tongue El Niño and warm pool El Niño, *J. Clim.*, *22*, 1499–1515, doi:10.1175/2008JCLI2624.1.

Lee, T., and M. J. McPhaden (2010), Increasing intensity of El Niño in the central-equatorial Pacific, *Geophys. Res. Lett.*, *37*, L14603, doi:10.1029/2010GL044007.

Lian, T., and D. Chen (2012), An evaluation of rotated EOF analysis and its application to tropical Pacific SST variability, *J. Clim.*, *25*, 5361–5373, doi:10.1175/JCLI-D-11-00663.1.

McPhaden, M. J. (1999), Climate oscillations: Genesis and evolution of the 1997–98 El Niño, *Science*, *283*, 950–954.

McPhaden, M. J. (2004), Evolution of the 2002/03 El Niño, *Bull. Am. Meteorol. Soc.*, *85*, 677–695.

Newman, M., S.-I. Shin, and M. A. Alexander (2011), Natural variation in ENSO flavors, *J. Geophys. Res.*, *38*, L14705, doi:10.1029/2011GL047658.

Penland, C., and P. D. Sardeshmukh (1995), The optimal growth of tropical sea surface temperature anomalies, *J. Clim.*, *8*, 1999–2024, doi:10.1175/1520-0442.

Périgaud, C., S. E. Zebiak, F. Mélin, J. P. Boulanger, and B. Dewitte (1997), On the role of meridional wind anomalies in a coupled model of ENSO, *J. Clim.*, *10*, 761–773.

Picaut, J., F. Masia, and Y. DuPenhoat (1997), An advective-reflective conceptual model for the oscillatory nature of the ENSO, *Science*, *277*, 663–666.

Rasmusson, E. M., and T. H. Carpenter (1982), Variations in tropical sea surface temperature and surface wind fields associated with the Southern Oscillation/El Niño, *Mon. Weather Rev.*, *110*, 354–384.

Rayner, N. A., D. E. Parker, E. B. Horton, C. K. Folland, L. V. Alexander, D. P. Rowell, E. C. Kent, and A. Kaplan (2003), Global analyses of sea surface temperature, sea ice, and night marine air temperature since the late nineteenth century, *J. Geophys. Res.*, *108*(D14), 4407, doi:10.1029/2002JD002670.

Saha, S., et al. (2005), The NCEP Cliamte Forecast System, *J. Clim.*, *15*, 3483–3517.

Vecchi, G., and D. Harrison (2000), Tropical Pacific sea surface temperature anomalies, El Niño, and equatorial westerly wind events, *J. Clim.*, *13*, 1814–1830.

Wyrtki, K. (1975), El Niño—The dynamic response of the equatorial Pacific Ocean to atmospheric forcing, *J. Phys. Oceanogr.*, *5*, 572–594.

Yeh, S.-W., J.-S. Kug, B. Dewitte, M.-H. Kwon, B. Kirtman, and F.-F. Jin (2009), El Niño in a changing climate, *Nature*, *461*, 511–514, doi:10.1038/nature08316.

Yu, J. Y., and S. T. Kim (2011), Identifying the types of major El Niño events since 1870, *Int. J. Climatol.*, *33*, 2105–2112.

Zebiak, S. E., and M. A. Cane (1987), A model El Niño–Southern Oscillation, *Mon. Weather Rev.*, *115*, 2262–2278.